

Many-body critical Casimir interactions in colloidal suspensions

Hendrik Hobrecht and Alfred Hucht

Fakultät für Physik and CENIDE, Universität Duisburg-Essen, D-47048 Duisburg, Germany

(Dated: August 3, 2022)

We study the fluctuation-induced Casimir interactions in colloidal suspensions, especially between colloids immersed in a binary liquid close to its critical demixing point. To simulate these systems, we present a highly efficient cluster Monte Carlo algorithm based on geometric symmetries of the Hamiltonian. Utilizing the principle of universality, the medium is represented by an Ising system while the colloids are areas of spins with fixed orientation. Our results for the Casimir interaction potential between two particles at the critical point perfectly agree with the exact predictions. However, we find that in finite systems the behavior strongly depends on whether the medium order parameter is conserved and zero, or is allowed to fluctuate. Finally we present first results for the three-body Casimir interaction potential.

PACS numbers: 64.60.De, 82.70.Dd, 05.70.Jk, 11.25.Hf

I. INTRODUCTION

Over the last few years colloidal suspensions have played a key role as experimental model systems for phase transitions and aggregation processes. Especially colloids immersed in a binary liquid have been investigated experimentally, since near the demixing transition of the solvent long-ranged correlated fluctuations give rise to critical Casimir forces. Those forces are peculiarly interesting for several qualities: Experimentally their sensitive temperature dependency allows to control the interaction strength *in situ* and reversibly. Furthermore the colloids can be observed directly with common microscopy methods. From a theoretical point of view, these critical Casimir forces are interesting because they are universal, i. e., different systems in the same universality class near their critical point show the very same behavior and share universal scaling functions.

Fluctuation-induced forces were first predicted by Casimir in 1948 [1]; he realized that the fluctuations of the electromagnetic field cause an attractive forces between two perfectly conducting plates in vacuum. Analogously, there are critical Casimir forces near a continuous phase transition in thermodynamic systems induced by the long-ranged correlated fluctuations of the order parameter if the medium is restricted by the systems geometry. An according theory was formulated in 1978 by Fisher and de Gennes for a system in d -dimensional slab geometry $L_{\perp} \times L_{\parallel}^{d-1}$ with $L_{\parallel} \gg L_{\perp}$ [2]. A first experimental proof of those forces has been given by Garcia and Chan; they observed a change in the thickness of critical liquid films of ^4He near its λ -point [3] and of ^3He - ^4He mixture near its tricritical point [4]. Binary liquids have also been studied in this geometry, extending the experiments to the Ising universality class [5]. Hertlein *et al.* reported the direct measurement of the critical Casimir force between a single colloid and a wall embedded in a binary liquid [6], which led to several other experiments on colloidal suspensions [7–10].

Since there are only a few simple systems for which the scaling functions are known exactly, e. g., the two-

dimensional Ising model [11, 12] or the large- n approach [13, 14], both in slab geometry, Monte Carlo (MC) studies of such critical systems have proven to be another tool to determine the characteristic universal behavior. Besides the MC simulations of the slab geometry, which all use some kind of thermodynamic integration to determine the scaling functions of the free energy and the Casimir force itself [15, 16], there are a few studies of the interaction between a spherical particle and a wall [17]. In a recent study we have shown how the thermodynamic integration can be avoided by allowing an object to move during the MC simulation and analyzing its distribution function [18]. This approach is therefore very similar to the experimental method of Hertlein [6], and it was used very recently to study the phase diagram of two-dimensional colloids [19].

As the Casimir forces are non-additive, describing their interactions with pair potentials is insufficient in systems with more than two particles, and higher-order contributions have to be taken into account. Unfortunately the common methods to simulate such systems with many-body interactions get inefficient or inaccurate the more bodies interact. Previous simulation studies [10, 18, 19] used standard local Monte Carlo algorithms, which suffer from the time-consuming effect of critical slowing down near the critical point and thus become very inefficient especially for large systems. This effect can be suppressed by using cluster algorithms; the probably most famous example is the Wolff algorithm [20], first introduced for the Ising model and based on the previous work by Swendsen and Wang [21]. While those algorithms utilize the Z_2 symmetry of the Hamiltonian and do not conserve the order parameter, Heringa and Blöte introduced an algorithm which uses the invariance of the Hamiltonian under some geometric transformations, e. g., a point reflection [22], builds two symmetric clusters and exchanges them under conservation of the order parameter. This geometric cluster algorithm (GCA) was later generalized to an off-lattice algorithm for spherical particles by Liu and Luijten, which builds two clusters of particles and exchanges them [23]. Therefor this generalized

geometric cluster algorithm (GGCA) reflects a particle at a pivot point and iteratively adds spheres to the cluster utilizing the hard-sphere potential, until a configuration without overlaps is generated. The cluster building process can be extended to include additional interactions between the particles.

In the present study we introduce a new MC cluster algorithm that is capable of both moving the particles and mixing the medium within one cluster step. We apply this algorithm to the two-dimensional Ising model in order to compare our results to the exactly known universal two-body interaction at criticality, calculated by Burkhardt and Eisenriegler [24] using conformal field theory [25]. Therefor we will introduce the common theoretical background, starting with the description of the critical Casimir effect in slab geometry and its connection to the fluctuation-induced force between two colloidal particles in a critical medium. Having recapitulated the exact results for the interaction potential scaling function, we explain our method to determine the potential itself using the two-particle correlation function. Afterwards we present the model we use to simulate the colloidal suspension. Then we describe the cluster algorithm and discuss the crucial modifications compared to the original GCA as well as its limiting cases. Eventually we compare our MC results for two interacting particles with the theory and discuss the unexpected result that in finite systems the scaling function strongly depends on whether the medium order parameter is allowed to fluctuate, or is conserved and fixed to zero during the simulation.

Finally we present first results for the three-body interactions. Therefor we show how the n -body correlation function and the n -body Casimir interaction potential are connected in general. We introduce the concept of an infinitely strong *ghost bond* between two particles acting as constraint to the possible particle motions. With this ghost bond we are able to considerably speed up the simulations. We present our MC results for the three-body interaction slightly above the critical temperature T_c , where we found it to be much stronger than directly at T_c . These results are obtained in a periodic $L \times L$ system with fluctuating order parameter. A comparison with zero-fixed medium magnetization will be presented elsewhere [26].

II. THEORY

Before we head for the critical Casimir interaction potential between two spherical objects, we start with a short repetition of the relevant quantities in the simpler slab geometry $L_\perp \times L_\parallel^{d-1}$ with periodic boundary conditions (BC) in the parallel directions and arbitrary BCs in perpendicular direction. The critical Casimir force per unit area $A = L_\parallel^{d-1}$ at reduced temperature $t = T/T_c - 1$

reads

$$\beta \mathcal{F}_C(t, L_\perp, L_\parallel) \equiv -\frac{1}{A} \frac{\partial}{\partial L_\perp} \delta F(t, L_\perp, L_\parallel), \quad (1)$$

with $\beta = 1/k_B T$, where the residual free energy δF , or *Casimir potential* in the context of colloidal suspensions, is given by

$$\delta F(t, L_\perp, L_\parallel) \equiv F(t, L_\perp, L_\parallel) - V f_b(t) - A f_s(t), \quad (2)$$

with total free energy $F(t, L_\perp, L_\parallel)$, bulk free energy density $f_b(t)$, surface free energy per unit area $f_s(t)$, and volume $V = L_\perp A$. All energies are in units of $k_B T$.

Fisher and de Gennes [2] proposed that the Casimir force fulfills the scaling *ansatz* [27]

$$\beta \mathcal{F}_C(t, L_\perp, L_\parallel) \simeq L_\perp^{-d} \vartheta^{ab}(x, \rho) \quad (3)$$

near the critical point, where a and b denote the surface preferences of the boundaries. Beneath those surface preferences, the universal scaling function ϑ^{ab} depends only on the temperature scaling variable x and on the given geometry, represented by the aspect ratio ρ ,

$$x = t \left(\frac{L_\perp}{\xi_0^+} \right)^{1/\nu}, \quad \rho = \frac{L_\perp}{L_\parallel}, \quad (4)$$

where ξ_0^+ is the correlation length amplitude above T_c , and ν is the critical exponent of the correlation length. Accordingly, the Casimir potential satisfies a similar *ansatz*

$$\delta F(t, L_\perp, L_\parallel) \simeq \Phi^{ab}(x, \rho), \quad (5)$$

where Φ^{ab} is again a universal scaling function.

Using this result for $\rho \rightarrow 0$ and the conformal invariance at criticality [25], Burkhardt and Eisenriegler calculated the asymptotics of the Casimir potential for two spherical objects in an infinitely large d -dimensional critical medium [24]. Analogously to the geometric scaling variable ρ in Eq. (4), they introduced the conformal invariant scaling variable

$$\kappa = \frac{r^2 - R_1^2 - R_2^2}{2R_1 R_2}, \quad (6)$$

where R_1 and R_2 are the radii of the two particles with surface preference a and b , respectively, and r is the distance between their centers. Thus the conformal scaling variable κ encodes both the relative positions and the sizes of the two spheres. Note that for the two-dimensional case the interaction between any two arbitrary shaped objects may be obtained exactly [28], as the group of conformal transformations is more powerful in $d = 2$.

For arbitrary d the Casimir potential scaling function of two spheres at the critical point fulfills

$$\Phi_c^{ab}(\kappa) \simeq \delta F_2(t=0, R_1, R_2; r) \quad (7)$$

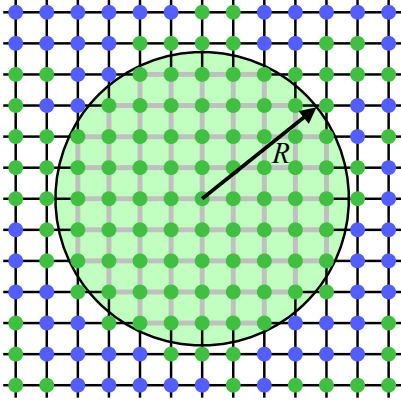


FIG. 1. (Color online) Embedment of a spherical particle with radius R onto the lattice. \uparrow and \downarrow spins are green (light) and blue (dark), respectively. Infinite strong couplings are grey, while normal bonds with strength K are shown black.

and asymptotically reads (Φ_c^{ab} is named \mathcal{F}_{ab} in [24])

$$\Phi_c^{ab}(\kappa) \stackrel{\kappa \rightarrow 1^+}{\simeq} \Delta_C^{ab} S_d [2(\kappa - 1)]^{-(d-1)/2} \quad (8)$$

for small distances $\kappa \rightarrow 1^+$, where S_d is the surface of the d -dimensional unit sphere and Δ_C^{ab} denotes the universal Casimir amplitude of the corresponding slab geometry. For the two-dimensional Ising case considered in this work $S_2 = 2\pi$ and $\Delta_C^{\uparrow\uparrow} = \Delta_C^{\circ\circ} = -\pi/48$.

In the limit of large distances between the two particles, i. e., for $\kappa \gg 1$, the Casimir potential behaves as

$$\Phi_c^{ab}(\kappa) \stackrel{\kappa \gg 1}{\simeq} - \sum_{\phi} Q_{\phi}^{ab} [2(\kappa + 1)]^{-x_{\phi}}, \quad (9)$$

where the sum is over all relevant scaling operators ϕ , e. g., for the Ising model the energy density ϵ and the magnetization density σ , with according scaling dimension x_{ϕ} . The amplitude ratios Q_{ϕ}^{ab} are universal and are known exactly for some special cases, e. g., the two-dimensional Ising class [24], where Eq. (9) simplifies to

$$\Phi_c^{\uparrow\uparrow}(\kappa \gg 1) \simeq -\sqrt{2}[2(\kappa + 1)]^{-1/8}, \quad (10a)$$

$$\Phi_c^{\circ\circ}(\kappa \gg 1) \simeq -[2(\kappa + 1)]^{-1}. \quad (10b)$$

For completeness we also give the exact scaling functions for the Ising case [28, 29],

$$\Phi_c^{ab}(\kappa) = \frac{\pi\rho}{12} - \ln \left[\sqrt{\frac{\vartheta_3(e^{-2\pi\rho})}{\eta(2i\rho)}} + s_{ab} \sqrt{\frac{\vartheta_2(e^{-2\pi\rho})}{\eta(2i\rho)}} \right]. \quad (11)$$

Here, $\kappa = \cosh(2\pi\rho)$ and $s_{ab} = \{1, 0, -1\}$ for BCs $ab = \{\uparrow\uparrow, \circ\circ, \uparrow\downarrow\}$, while $\vartheta_j(q)$ and $\eta(\tau)$ denote the Jacobi theta functions and the Dedekind eta function, respectively.

The reversible work theorem [30] states that the residual free energy $\delta F_2(r)$ is directly related to the two-particle distribution function $g_2(r)$ by

$$g_2(t, R_1, R_2; r) = e^{-\delta F_2(t, R_1, R_2; r)}. \quad (12)$$

Note that in the bulk $\delta F_2(r \rightarrow \infty) = 0$ and $g_2(r \rightarrow \infty) = 1$ by definition. If the system is at its critical point, we can use Eqs. (7) and (12) to calculate the corresponding Casimir potential scaling function

$$\Phi_c^{ab}(\kappa) \simeq -\ln g_2(t=0, R_1, R_2; r), \quad (13)$$

and hence we can determine $\Phi_c^{ab}(\kappa)$ from a measurement of the two-particle distribution function $g_2(r)$. The results of this analysis are presented in Section IV.

III. MODEL AND CLUSTER ALGORITHM

We model the binary liquid using an Ising system with the Hamiltonian, in units of $k_B T$,

$$\mathcal{H} = - \sum_{\langle ij \rangle} K_{ij} s_i s_j \quad (14)$$

on a simple cubic lattice in d dimensions with L^d spins and periodic BCs in all directions. The reduced couplings $K_{ij} \geq 0$ are assumed to be ferromagnetic, and the sum runs over all nearest neighbor pairs $\langle ij \rangle$. Analogous to a lattice-gas interpretation, the spins pointing up ($s = \uparrow$) or down ($s = \downarrow$) may be understood as particles of species A or B , respectively. The critical composition for this system is a ratio of $A:B = 1:1$, i. e., at total medium magnetization $M = 0$.

Now we insert N spherical particles with radius R_{μ} located at positions \mathbf{r}_{μ} , $\mu = 1, \dots, N$, into the system. Each particle is realized as a group of spins at position \mathbf{r} fulfilling $|\mathbf{r} - \mathbf{r}_{\mu}| < R_{\mu}$, aligned in the same direction by virtue of infinitely strong couplings according to

$$K_{ij} = \begin{cases} \infty & \text{if } s_i \text{ and } s_j \text{ belong to one particle,} \\ K & \text{else.} \end{cases} \quad (15)$$

For a more complex model one could also distinguish between particle-medium couplings and the coupling between two different particles at the particle surfaces.

Apart from the nearest neighbor couplings K_{ij} between the spins there are no other particle interactions. Instead, these interactions are induced by the correlated medium, and thus not only the Casimir pair interaction, but all fluctuation induced many-body interactions are included automatically.

We now modify the GCA by Heringa and Blöte and explicitly include the bonds $\langle ij \rangle$ with couplings K_{ij} into the cluster building process. In this way the particles encoded into the bonds will also be moved by the cluster algorithm. We assume that neighboring lattice sites i and j as well as the connecting bond $\langle ij \rangle$ are mapped onto the sites i' and j' and the bond $\langle i'j' \rangle$, respectively. Furthermore we assume a point reflection with respect to a pivot as symmetry operation.

The energy difference of an exchange of the two spins s_j and $s_{j'}$ due to activation of the bond pair $\langle ij \rangle$ and

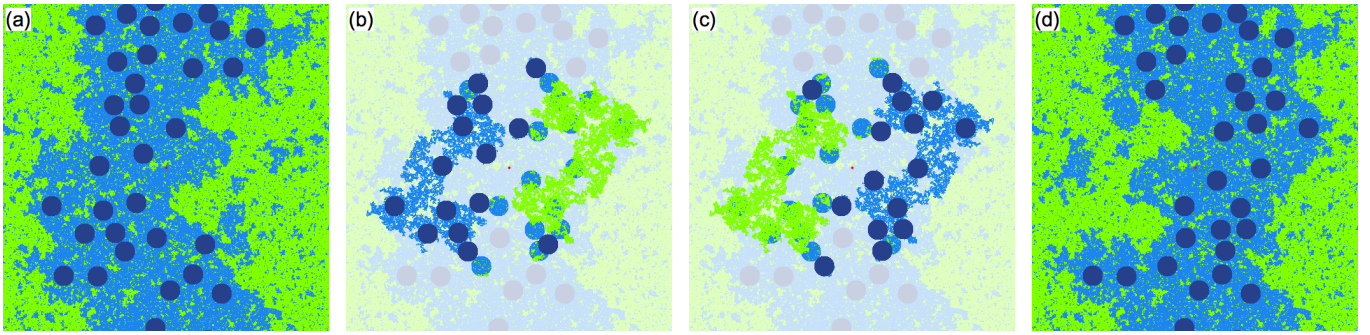


FIG. 2. (Color online) One typical cluster spin flip in a periodic two-dimensional system with linear size $L = 512$ and $N = 32$ particles with radius $R = 16$ and \uparrow surface preference at T_c . Up (Down) medium spins are shown in blue (light green). The medium magnetization is fixed to $M = 0$ and the pivot (red point) is in the center of the figures. Starting from an initial configuration (a) two clusters are built symmetrically around the pivot (b) and are exchanged (c), leading to a new equilibrium configuration (d).

$\langle i'j' \rangle$ is given by

$$\Delta E = K_{ij}s_i s_j + K_{i'j'}s_{i'} s_{j'} - K(s_i s_{j'} + s_{i'} s_j), \quad (16)$$

where the cases of infinite couplings, Eq. (15), are accounted for by the coupling K in the last term. The algorithm can be summarized as follows:

1. Choose two different random lattice sites i and i' and use them as starting points for the two clusters \mathcal{C} and \mathcal{C}' . Set the pivot to the midpoint of i and i' . Put (i, i') on the stack (a list of lattice site pairs).
2. Read a pair (i, i') from the stack. For all neighbor sites (j, j') of (i, i') calculate ΔE [Eq. (16)] and, if $\Delta E > 0$, do the following with probability $P_{\text{add}} = 1 - e^{-\Delta E}$:
 - (a) Add the bonds $\langle ij \rangle$ and $\langle i'j' \rangle$ to \mathcal{C} and \mathcal{C}' if not already added.
 - (b) If (j, j') are not already added to the clusters, add them to \mathcal{C} and \mathcal{C}' and put them on the stack.
3. Execute step (2) until the stack is empty.
4. Exchange the clusters \mathcal{C} and \mathcal{C}' .

Note that step 4 can be eliminated, as the spin and bond exchange can already be performed during the cluster building process. Furthermore, it is sufficient to put spin i on the stack and to calculate i' using the pivot.

If both s_i and s_j or both $s_{i'}$ and $s_{j'}$ belong to one particle, the energy difference $\Delta E = \infty$ and thus $P_{\text{add}} = 1$, which ensures that particles are always added as a whole and that there are only bonds with coupling K at the edges of the two clusters. Thus the proof of detailed balance follows just the one for the GCA [22] with the energy $\Delta E = K(s_i - s_{i'})(s_j - s_{j'})$ for activating an edge bond. Note that the activated bonds within the clusters, especially all bonds of a particle, are exchanged, too, so the particles do not fall apart.

If no particles are initialized, this algorithm is identical to the original GCA, which has its percolation threshold at the critical point and thus suppresses the effect of critical slowing down very efficiently. Additionally, there

is a second limiting case: for infinite high temperature $K = 0$ in Eq. (15) this algorithm is a lattice version of the GGCA by Liu and Luijten [23], since for this case the medium is not correlated anymore and the particles do only interact with a hard-sphere potential.

It is straightforward to include walls as lines of infinitely coupled \uparrow or \downarrow spins into the algorithm similar to Ref. [18]. Furthermore, we can include arbitrary particle-particle couplings as long-ranged bonds with strength $K_{\mu\nu}(\mathbf{r}_\mu, \mathbf{r}_\nu)$, as proposed in Ref. [23].

In the following sections we use this algorithm to investigate a two-dimensional system with N identical spherical particles with \uparrow surface preference. We first turn to the...

IV. TWO-PARTICLE INTERACTION

By analyzing the two-particle distribution function $g_2(r)$ of the particles at criticality and sufficiently low particle densities $\varrho \equiv N\pi R^2/L^2$, we obtained the Casimir potential $\delta F_2(r)$ using Eq. (12) and compared it with the exact scaling function $\Phi_c^{ab}(\kappa)$ for $\varrho \rightarrow 0$. For the near field asymptotics $\kappa \lesssim 2$ we studied a system with $N = 2$ particles having radius $R = 64$ on a $L = 512$ square lattice ($\varrho = \pi/32$). For larger distances $\kappa \gtrsim 2$ we simulated systems on $L = \{128, 256, 512\}$ lattices with $N = \{2, 8, 32\}$ particles, respectively, all with radius $R = 8$, so that these systems share a constant particle density $\varrho = \pi/128$. To determine the Casimir potential we made a histogram of the particle distances, based on at least 6 million independent particle positions, and calculated the discrete two-dimensional two-particle distribution function $g_2(\mathbf{r}_{12})$, where $\mathbf{r}_{\mu\nu} = \mathbf{r}_\nu - \mathbf{r}_\mu$ denotes the discrete distance vector between the centers of two particles μ and ν . We used the distance vector \mathbf{r}_{12} instead of the scalar distance r in order to account for lattice anisotropies. Then we assigned the appropriate value of the conformal invariant scaling variable κ , Eq. (6), to each point of $g_2(\mathbf{r}_{12})$. The leading lattice dis-

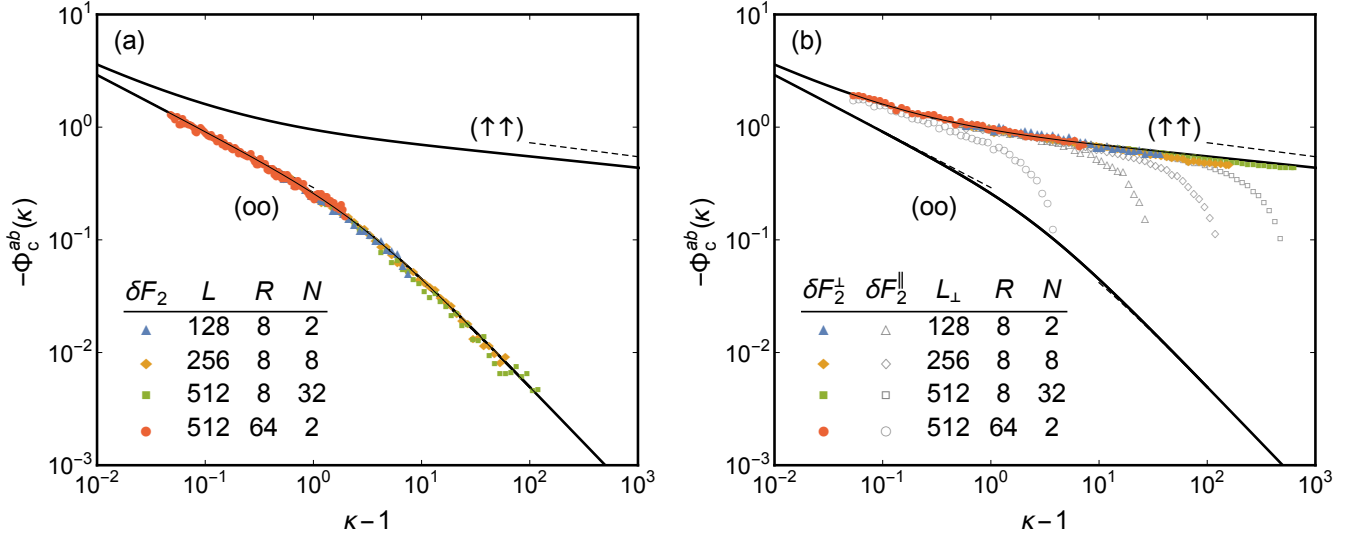


FIG. 3. (Color online) Two-particle Casimir potential $\Phi_c^{ab}(\kappa)$ between $N \uparrow$ spheres with radius R embedded into a critical medium of size L^2 with fluctuating order parameter (a), as well as for a rectangular medium with fixed order parameter $M = 0$ (b). In the latter case we fixed the aspect ratio to $\rho = 1/2$ in order to induce defined domain walls in \perp direction and independently measured the potential in \perp and \parallel directions. The data points are $-\delta F_2(r)$ from the simulations, Eq. (12), while the solid lines are calculated using Eq. (11), and the dashed lines are the asymptotes from Eqs. (8) and (10). Due to the finite system size L the spheres polarize the medium in case (a), leading to an effective open boundary condition at the sphere surfaces and consequently to a data collapse onto the scaling function $\Phi_c^{oo}(\kappa)$. The expected scaling behavior, with scaling function $\Phi_c^{\uparrow\uparrow}(\kappa)$, is only found if the medium polarization is suppressed (b). In this case, finite-size corrections due to the two domains occur that are efficiently controlled through the rectangular geometry. They are only visible in \parallel direction, where they lead to a sign change in $\delta F_2^{\parallel}(r \approx L_{\perp})$, while the data for $\delta F_2^{\perp}(r)$ nicely collapses onto the scaling function $\Phi_c^{\uparrow\uparrow}$ for all r .

cretization effects are corrected with an effective radius $R_{\text{eff}} = R + \delta R$ for the spheres, with $\delta R = -0.9(1)$, as proposed in Refs. [17, 18]. Additionally, we used a logarithmic binning in $\kappa - 1$ for the data to obtain equidistant points in the double logarithmic scale and for sake of a better statistic. With the MC data we were able to cover a range of approximately $\kappa - 1 \in [10^{-2}, 10^3]$. After having obtained the two-particle distribution function, we finally used Eq. (12) to determine the interaction potential $\delta F_2(r)$. Note that the results for $R = 64$ were corrected for excluded volume effects by dividing g_2 by $1 - 8\pi R^2/V$, a term which turns out to be negligible for $R = 8$.

As it is common to study systems with a fluctuating instead of a fixed order parameter, we combined our cluster algorithm with Wolff cluster updates for the spin medium. In this context one would expect the determined potentials $\delta F_2(r)$ to fall on the predicted curves for the symmetry-breaking surface preferences $\Phi_c^{\uparrow\uparrow}(\kappa)$, but surprisingly we find them to agree with the scaling function $\Phi_c^{oo}(\kappa)$ for open boundary conditions, as shown in Fig. 3a. This kind of behavior can, however, be understood: The particles act as surface magnetic fields, forcing the surrounding medium to form a domain with the same orientation, which is described by the decay of magnetization profile around such a particle proportional to $r^{-1/4}$ as derived in [31]. Due to this slow decay and the periodic boundary conditions, finite size effects of the

order of $L^{-1/8}$ occur (see below). The system size is way too small to show bulk behavior, and the whole system is forced to polarize as illustrated in Fig. 4a. Thus this deviation from the expected behavior is a finite-size effect, which should vanish only for much larger systems. Because large parts of the system have the same orientation as the particles, they have effective open boundary conditions and the interaction potential reflects this with a faster decay.

In order to resolve this discrepancy, we performed another set of simulations with fixed total medium magnetization $M = 0$, using only the described cluster algorithm and no Wolff updates. As we now force two domains into the system, it turns out to be beneficial to change the systems aspect ratio from $\rho = 1$ to $\rho = 1/2$, i. e., $L_{\parallel} = 2L_{\perp}$, as then two dominant domains fit into the system, see Fig. 4b. Since the system tries to minimize the length of the domain walls, it is most likely to find the domains separated along the parallel direction. Thus the system is highly anisotropic with respect to the parallel and the perpendicular directions, and we can measure the two-particle distribution function in the two directions independently. We restrict our analysis of the two-particle distribution function to parallel and perpendicular strips with width $2R$ around the symmetry axes of the system centered in the middle of the exclusion volume, shown as dotted lines in Fig. 5. We used the same parameters as before, i. e., $N = \{2, 8, 32\}$ particles, all having radius

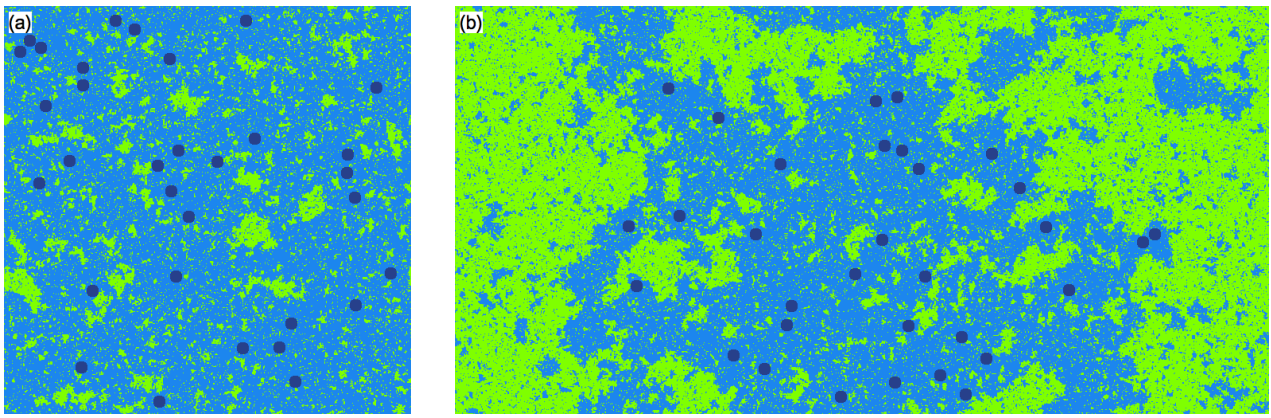


FIG. 4. (Color online) Typical configurations with fluctuating (a) and with fixed (b) magnetization in periodic systems with $L_{\perp} = 512$ and $N = 32$ particles with radius $R = 8$ and \uparrow surface preference at T_c . The strong polarization in case (a) leads to effective open boundary condition at the spheres. In case (b), on the other hand, the two dominant domains present in the system lead to more realistic critical domain structures.

$R = 8$, for $L_{\perp} = \{128, 256, 512\}$, respectively, and $N = 2$ particles with radius $R = 64$ in a system with $L_{\perp} = 512$, all at criticality. Note that the effective particle density ϱ in the \uparrow phase is unchanged.

Now the resulting Casimir potentials $\delta F_2^{\perp, \parallel}(r)$ in *both* directions show the expected scaling behavior at least at small distances and nicely agree with the exact scaling function $\Phi_c^{\uparrow\uparrow}(\kappa)$ for equal symmetry breaking surface preferences, see Fig. 3b. For the perpendicular case, $\delta F_2^{\perp}(r)$ perfectly agrees with the exact result up to the largest possible distances, while the Casimir potential $\delta F_2^{\parallel}(r)$ shows a drop-off for large κ , marked as gray symbols in Fig. 3b. This is a consequence of the domain with opposite orientation caused by the conserved order parameter, which leads to an effectively repulsive force onto the particles. The cutoff at $r \approx L_{\parallel}/2$ follows from a change of sign in the potential due to this anti-correlation between the particles and the domain with opposite orientation, see Fig. 5. The deviation from the predicted curve starts at about half this cutoff distance.

To understand the cross-over between the two cases, we additionally performed simulations with $L = 128$ and $R = 8$ at different fixed magnetizations $M > 0$. We found results that continuously interpolate between the two scaling functions $\Phi_c^{\circ\circ}$ and $\Phi_c^{\uparrow\uparrow}$. While for $M \lesssim 1/16$ we see no differences from the $M = 0$ curves, for $M_{\circ\circ} = 0.6$ the data agree with $\Phi_c^{\circ\circ}$. For $M_{\times} = 1/8$ the results fall onto $\Phi_c^{\uparrow\uparrow}$ for $\kappa \lesssim 2$ and then decay similar to $\Phi_c^{\circ\circ}$. Combining these results with the fact that the critical magnetization in finite systems scales proportionally to $L^{-1/8}$ we conclude that in systems with fluctuating order parameter a linear system size of $L_{\times} = (M_{\circ\circ}/M_{\times})^8 L \approx 3.6 \times 10^7$ would be necessary to reach the correct scaling behavior in the cross-over region $\kappa \approx 2$.

Another effect the data show is the better statistics for the simulations with conserved order parameter. This stresses that our algorithm works best at a total magnetization $M = 0$. During the simulation with the combi-

nation of algorithms, there are fewer and smaller pairs of clusters with opposite orientation there and thus the algorithm gets less effective and the autocorrelation time grows.

V. THREE-PARTICLE INTERACTION

If a third particle is getting close to two others, the pairwise description fails and three-body contributions become relevant because of the non-additive character of the critical Casimir force. In analogy to the two particle case, Eq. (12), this effect can be characterized by the according n -point distribution function $g_n(\mathbf{r}_1, \dots, \mathbf{r}_n)$. The function g_n is directly related to the n -particle Casimir potential δF_n via the reversible work theorem [30],

$$g_n(\mathbf{r}_1, \dots, \mathbf{r}_n) = e^{-\delta F_n(\mathbf{r}_1, \dots, \mathbf{r}_n)}, \quad (17)$$

and δF_n can be decomposed into pure k -particles contributions δf_k according to

$$\begin{aligned} \delta F_n(\mathbf{r}_1, \dots, \mathbf{r}_n) &= \sum_{\substack{\mu, \nu=1 \\ \mu < \nu}}^n \delta f_2(\mathbf{r}_{\mu}, \mathbf{r}_{\nu}) \\ &+ \sum_{\substack{\mu, \nu, \lambda=1 \\ \mu < \nu < \lambda}}^n \delta f_3(\mathbf{r}_{\mu}, \mathbf{r}_{\nu}, \mathbf{r}_{\lambda}) + \dots \end{aligned} \quad (18)$$

Note that $\delta F_N(\mathbf{r}_1, \dots, \mathbf{r}_{\mu}, \dots, \mathbf{r}_N)$ is the change in the total free energy of a system with N particles if particle μ is added to the system from infinite distances.

We again assume translational invariance, with distance vectors $\mathbf{r}_{\mu\nu} = \mathbf{r}_{\nu} - \mathbf{r}_{\mu}$, and consequently all n -point functions depend on $n - 1$ distances. For $n = 2$ we get $\delta F_2(\mathbf{r}_{12}) = \delta f_2(\mathbf{r}_{12})$ and recover Eq. (12), while the three-particle Casimir potential decomposes to

$$\begin{aligned} \delta F_3(\mathbf{r}_{12}, \mathbf{r}_{13}) &= \delta f_2(\mathbf{r}_{12}) + \delta f_2(\mathbf{r}_{13}) + \delta f_2(\mathbf{r}_{23}) \\ &+ \delta f_3(\mathbf{r}_{12}, \mathbf{r}_{13}). \end{aligned} \quad (19)$$

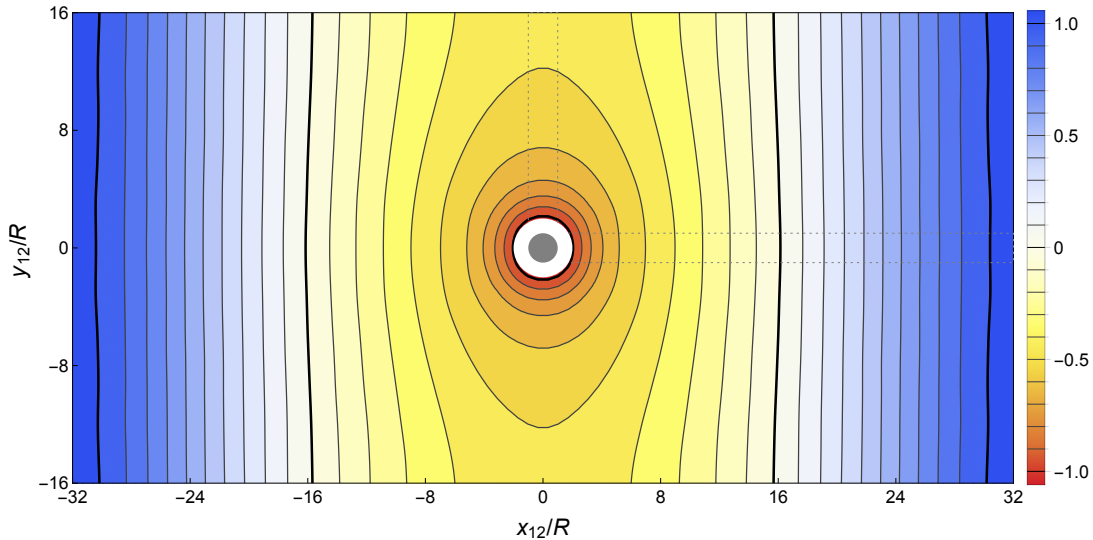


FIG. 5. (Color online) Contour plot of the two-particle Casimir potential $\delta F_2(\mathbf{r}_{12})$ as determined from the Monte Carlo simulations. We show data for a system with $L_\perp = 256$ and $L_\parallel = 512$ and fixed medium magnetization $M = 0$. In the system are $N = 8 \uparrow$ particles with radius $R = 8$. The white region in the center is the exclusion volume, and the reference particle is shown as gray disk. The regions used for the determination of the scaling functions is marked with dotted lines. The underlying histogram of $g_2(\mathbf{r}_{12})$ contains 672 million entries.

Therefore, the pure three-particle contribution can be calculated as

$$\delta f_3(\mathbf{r}_{12}, \mathbf{r}_{13}) = -\ln \left[\frac{g_3(\mathbf{r}_{12}, \mathbf{r}_{13})}{g_2(\mathbf{r}_{12})g_2(\mathbf{r}_{13})g_2(\mathbf{r}_{23})} \right] \quad (20)$$

and requires the calculation of a four-dimensional histogram of the distances $g_3(\mathbf{r}_{12}, \mathbf{r}_{13})$ in $d = 2$ space dimension, which has to be accurately determined in the Monte Carlo simulations. As such a histogram needs a lot of memory storage, it would limit our studies to small systems or to a lower resolution for the particle positions. For a system with $L = 256$ a naive approach would be to use an array with $(L/2)^4$ entries, which would require about 1GB of memory storage. Furthermore, to acquire a reasonable statistics we need, say, 100 entries in each histogram bin on average, leading to $\approx 10^{10}$ independent measurements for $L = 256$. To considerably reduce the needed storage and simulation time we fixed the distance between the two particles 1 and 2, $\mathbf{r}_{12} = \text{const.}$, via a *ghost bond* between them, i.e., an additional infinitely strong coupling between the spins at the center of each particle. Indeed this is a simple version of the additional interaction introduced in the GGCA, and it does not change the condition of detailed balance, because still only the spins at the edge of the clusters contribute to the energy difference. Those ghost bonds fix the position of two particles and thus reduces the measurable distribution to one slice of the original histogram. With this approach we are able to avoid a lot of configurations where the three-particle correlation is very small, e.g., when one particle is far away from the other two, which results in a better statistic and thus reduces the simulation time enormously.

We simulated a system with fluctuating order parameter and $L = 256$, $R = 16$ and $N = 3$ in the constellation with two particles at their closest approach coupled via a ghost bond, $\mathbf{r}_{12} = (2R, 0)$, and the third particle free to move independently. At criticality we found that the three-particle correlation nearly vanishes even at the closest approach of all three particles. Thus we increased the temperature slightly above criticality and found a maximum of the correlation near $t = 0.025$, which is in qualitative agreement with the existence of a maximum of the Casimir interaction scaling function for $\uparrow\uparrow$ boundary conditions in slab geometry above T_c [11]. Figure 6a shows the resulting interaction potential $\delta F_3(\mathbf{r}_{12}, \mathbf{r}_{13})$, while the pure three-body contribution $\delta f_3(\mathbf{r}_{12}, \mathbf{r}_{13})$ according to Eq. (20) is shown in Fig. 6b. Just as expected the pure three-body potential $\delta f_3(\mathbf{r}_{12}, \mathbf{r}_{13})$ vanishes if the third particle moves away from the other two, while $\delta f_3(\mathbf{r}_{12}, \mathbf{r}_{13})$ becomes positive as the third particle gets close to the other two, leading to a repulsive contribution to the three-body Casimir force. Since the three-body interaction potential $\delta F_3(\mathbf{r}_{12}, \mathbf{r}_{13})$ is negative everywhere, the three particles still attract each other, but not as much as a superposition of the two-body interactions would predict. This result is similar to the experimental measurement of three-body interactions by Brunner *et al.* [32]; they studied a system of three charged colloids with a repulsive electrostatic interaction. Although the three-body interaction was repulsive, too, the pure three-body interaction was attractive and thus showed just the opposite behavior as the two-body interactions.

An explanation of this effect is that as the particle get closer, the fluctuating medium between the particles is displaced and thus there are less fluctuations to mediate

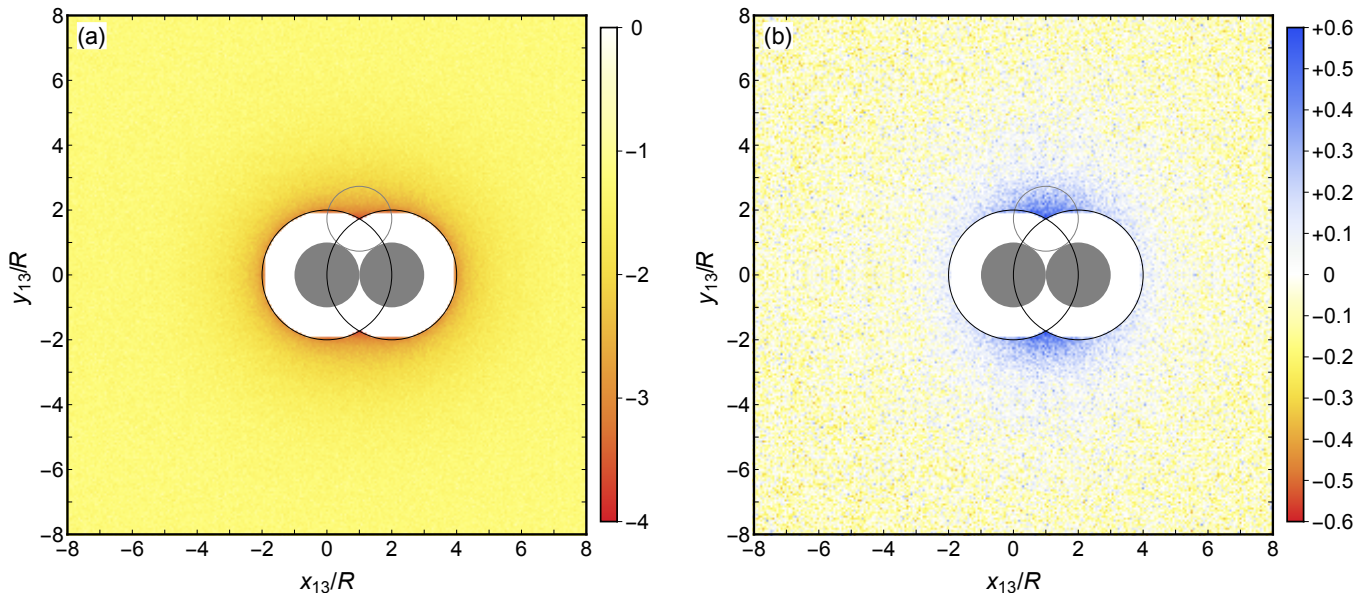


FIG. 6. (Color online) Three particle Casimir potential for a system with $L = 256$ and $N = 3$ particles having radius $R = 16$ at temperature $t = 0.025$ slightly above T_c . The first two particles (marked as gray discs) are fixed at their closest distance $\mathbf{r}_{12} = (2R, 0)$ as described in the text, while the third particle is allowed to move freely. The exclusion volume is shown with black circles, while one possible position of the third particle is shown as gray circle. (a) The Casimir potential $\delta F_3(\mathbf{r}_{12}, \mathbf{r}_{13})$ according to Eq. (19) is negative in the whole system, so the three particles attract each other, leading to a high probability of agglomeration. (b) The pure three-body contribution $\delta f_3(\mathbf{r}_{12}, \mathbf{r}_{13})$, calculated with Eq. (20), is repulsive at short distances \mathbf{r}_{13} and vanishes as the distance between the third particle and the other two increases.

the interactions, which leads to a reduction of the (attractive) force. That the three-body interaction has a maximum in a triangular configuration emphasizes this picture, since then the particles have the closest possible packing (marked as gray circles in Fig. 6).

VI. CONCLUSIONS

We presented a highly efficient cluster MC algorithm for the simulation of colloids immersed in a binary liquid, based on the geometric cluster algorithm by Heringa and Blöte [22]. The algorithm suppresses the effects of critical slowing-down near criticality at least at sufficiently low particle densities. It can be extended to contain additional interactions between the particles, such as electrostatic forces as present in experiments. We used this algorithm to calculate the critical two-particle Casimir potential $\delta F_2(r)$ over a range in the distance r that governs four orders of magnitude in the according conformal invariant scaling variable κ . As a surprising result we found a strong dependency on whether the medium order parameter is conserved and zero, or is allowed to fluctuate. In the latter case our MC results are in perfect agreement with the predictions for the critical Casimir interaction potential scaling function $\Phi_c^{\text{co}}(\kappa)$ between two particles with open boundaries, while in the former case the simulation agrees excellently with the scaling function $\Phi_c^{\uparrow\uparrow}(\kappa)$ predicted for equal symmetry-breaking boundary condi-

tions [24]. The deviating behavior can be understood as a finite-size effect and is related to the strong polarization of the medium in periodic systems at criticality. We could show that this effect can be suppressed using a fixed magnetization $M = 0$. The inevitable domain structure could be controlled by simulating rectangular systems with an aspect ratio $\rho = 1/2$.

Finally we presented first results for the three-body Casimir potential $\delta F_3(\mathbf{r}_{12}, \mathbf{r}_{13})$. We could significantly speed up the determination of the required three particle correlation function $g_3(\mathbf{r}_{12}, \mathbf{r}_{13})$ by introducing a ghost bond between particles 1 and 2, fixing their distance vector \mathbf{r}_{12} to the smallest possible value. The results show the same qualitative behavior as experiments on similar systems [32], as the full three-particle interaction is smaller than a two-particle picture would predict. Further studies are necessary to get a deeper understanding of the fluctuation-induced many-particle effects in colloidal suspensions, especially with conserved order parameter [26], where we expect stronger interactions analogously to the two-particle case.

ACKNOWLEDGMENTS

We wish to thank F. M. Schmidt, M. Hasenbusch and H. W. Diehl for fruitful discussions. This work was supported by the Deutsche Forschungsgemeinschaft through Grant No. HU 2303/1-1.

-
- [1] H. B. G. Casimir, Proc. K. Ned. Akad. Wet. **51**, 793 (1948).
- [2] M. E. Fisher and P.-G. de Gennes, C. R. Acad. Sci. Paris, Ser. B **287**, 207 (1978).
- [3] R. Garcia and M. H. W. Chan, Phys. Rev. Lett. **83**, 1187 (1999).
- [4] R. Garcia and M. H. W. Chan, Phys. Rev. Lett. **88**, 086101 (2002).
- [5] M. Fukuto, Y. F. Yano, and P. S. Pershan, Phys. Rev. Lett. **94**, 135702 (2005).
- [6] C. Hertlein, L. Helden, A. Gambassi, S. Dietrich, and C. Bechinger, Nature **451**, 172 (2008).
- [7] F. Soyka, O. Zvyagolskaya, C. Hertlein, L. Helden, and C. Bechinger, Phys. Rev. Lett. **101**, 208301 (2008).
- [8] D. Bonn, J. Otwinowski, S. Sacanna, H. Guo, G. Wegdam, and P. Schall, Phys. Rev. Lett. **103**, 156101 (2009).
- [9] O. Zvyagolskaya, A. J. Archer, and C. Bechinger, EPL (Europhysics Letters) **96**, 28005 (2011).
- [10] M. T. Dang, A. V. Verde, V. D. Nguyen, P. G. Bolhuis, and P. Schall, The Journal of Chemical Physics **139**, 094903 (2013).
- [11] R. Evans and J. Stecki, Phys. Rev. B **49**, 8842 (1994).
- [12] A. Hucht, D. Grüneberg, and F. M. Schmidt, Phys. Rev. E **83**, 051101 (2011), arXiv:1012.4399.
- [13] H. W. Diehl, D. Grüneberg, M. Hasenbusch, A. Hucht, S. B. Rutkevich, and F. M. Schmidt, EPL **100**, 10004 (2012), arXiv:1205.6613.
- [14] H. W. Diehl, D. Grüneberg, M. Hasenbusch, A. Hucht, S. B. Rutkevich, and F. M. Schmidt, Phys. Rev. E **89**, 062123 (2014), arXiv:1402.3510.
- [15] A. Hucht, Phys. Rev. Lett. **99**, 185301 (2007).
- [16] O. Vasilyev, A. Gambassi, A. Maciolek, and S. Dietrich, Phys. Rev. E **79**, 041142 (2009).
- [17] M. Hasenbusch, Phys. Rev. E **87**, 022130 (2013).
- [18] H. Hobrecht and A. Hucht, EPL **106**, 56005 (2014), arXiv:1405.4088.
- [19] J. R. Edison, N. Tasios, S. Belli, R. Evans, R. van Roij, and M. Dijkstra, Phys. Rev. Lett. **114**, 038301 (2015).
- [20] U. Wolff, Phys. Rev. Lett. **62**, 361 (1989).
- [21] R. H. Swendsen and J.-S. Wang, Phys. Rev. Lett. **58**, 86 (1987).
- [22] J. R. Heringa and H. W. J. Blöte, Phys. Rev. E **57**, 4976 (1998).
- [23] J. Liu and E. Luijten, Phys. Rev. Lett. **92**, 035504 (2004).
- [24] T. W. Burkhardt and E. Eisenriegler, Phys. Rev. Lett. **74**, 3189 (1995).
- [25] J. Cardy, J. Phys A: Math. Gen. **17**, L385 (1984).
- [26] H. Hobrecht and A. Hucht, to be published.
- [27] Throughout this work, the symbol \simeq means asymptotically equal in the respective limit, e.g., $f(L) \simeq g(L) \Leftrightarrow \lim_{L \rightarrow \infty} f(L)/g(L) = 1$.
- [28] G. Bimonte, T. Emig, and M. Kardar, EPL (Europhysics Letters) **104**, 21001 (2013).
- [29] J. Cardy, in Encyclopedia of Mathematical Physics, edited by J.-P. Francoise, G. L. Naber, and T. S. Tsun (Academic Press, Oxford, 2006) pp. 333 – 340.
- [30] D. Chandler, Introduction to Modern Statistical Mechanics (Oxford University Press, 1987).
- [31] T. W. Burkhardt and E. Eisenriegler, Journal of Physics A: Mathematical and General **18**, L83 (1985).
- [32] M. Brunner, J. Dobnikar, H.-H. von Grünberg, and C. Bechinger, Phys. Rev. Lett. **92**, 078301 (2004).